Cancer Letters 446 (2019) 81–89

Contents lists available at ScienceDirect

Cancer Letters

journal homepage: www.elsevier.com/locate/canlet

Original Articles

miR-140-3p functions as a tumor suppressor in squamous cell lung cancer by regulating BRD9

Haitao Huang[a,1], Yuxuan Wang[a,1], Qin Li[b,c,1], Xiaoyan Fei[b], Haitao Ma[a,*], Rongkuan Hu[b,**]

[a] Department of Thoracic Surgery, The First Affiliated Hospital of Soochow University, Suzhou, 215006, China
[b] Hefei National Laboratory for Physical Sciences at Microscale, School of Life Sciences, University of Science & Technology of China, Hefei, 230026, China
[c] School of Life Sciences and Biotechnology, Shanghai Jiao Tong University, Shanghai, 200240, China

ARTICLE INFO

Keywords:
microRNA
Bromodomain-containing protein
c-myc
Patient-derived xenograft
Tumorigenesis

ABSTRACT

Squamous cell lung cancer (SqCLC) is among the most malignant lung cancers worldwide, lacking biomarkers for diagnostic and targets for treatment. In this study, we observed that miR-140-3p was expressed at low levels both in SqCLC cell lines and patient samples, while overexpression of miR-140-3p dramatically reduced the cell proliferation and invasion in SqCLC cells and Patient derived xenograft (PDX) models. Our further investigation indicated miR-140-3p negatively affected the tumorigenesis of SqCLC by down-regulating the expression of BRD9, an oncogene in SqCLC. Inhibition of BRD9 repressed SqCLC tumorigenesis by regulating c-myc expression. Meanwhile, BRD9 expression is up-regulated and negatively correlated with miR-140-3p in clinical samples; a meta-analysis of survival data indicates that SqCLC patients with high levels of BRD9 in their tumors have a worse prognosis. Collectively, our study suggests the prognostic and therapeutic roles of miR-140-3p and BRD9 axis in squamous cell lung cancer.

1. Introduction

Squamous cell lung cancer (SqCLC) is a set of devastating diseases, which comprise approximately 30% of invasive non-small cell lung cancers (NSCLC) [1]. There remains no efficient targeted treatment for SqCLC, and platinum-based regimens are a standard clinical therapy for this devastating disease [2]. Early diagnosis of SqCLC is one of the most important factors contributing to successful and effective treatment. However, many patients are diagnosed with SqCLC due to the asymptomatic features of the early stages, resulting in a very late diagnosis and following low survival rates. Therefore, it is essential to identify SqCLC-specific molecular biomarkers for early diagnosis and treatment.

SqCLC development has been defined as a multistep process including accumulated genetic modifications and chronic inflammation due to smoking [3]. Moreover, the posttranscriptional regulation of tumors was lately recognized as the product of a developing crosstalk between different cell types. This posttranscriptional regulation includes a large set of noncoding RNAs, including microRNAs (miRNAs), circRNAs and lncRNAs [4]. MiRNAs are approximately 22-nucleotide RNAs that modulate essential cellular processes in many types of cancer. MiRNAs bind to the 3′ UTR and can regulate hundreds of mRNAs to play a critical role in a wide range of cellular processes. Many studies have indicated that miRNA levels are altered in lung cancer and that these miRNAs regulate cell growth and migration. These miRNAs thus act as tumor suppressors or oncogenes. For example, our previous study indicated that miR-342-3p is involved in the regulation of cell proliferation and invasion in non-small cell lung cancer (NSCLC) by targeting AGR2 [5]. Chen et al. reported that miR-30d-5p inhibits non-small cell lung cancer proliferation and motility by regulating CCNE2 [6]. MiR-29b mediates the NF-kB pathway in non-small cell lung cancers [7]. Very recently, miR-140 was reported to regulate PD-L1 in NSCLC, especially in adenocarcinoma lung cancers [8]. In addition, miR-140-3p was found to be downregulated in lung squamous cell carcinoma [9]. The function and detailed mechanism of miR-140 in SqCLC, however, remain unknown.

To further investigate potential pathways, several prediction algorithms were utilized to predict the target of miR-140-3p (Targetscan, miRDB and miRBase). Cross-reference analysis indicated that BRD9 is a direct target. BRD9 contains a bromodomain and regulates chromatin remodeling and transcription. It has been identified as a subunit of the BAF (SWI/SNF) nucleosome remodeling complex and plays a role in histone acetylation [10,11]. BRD9 is always overexpressed in several

* Corresponding author. 188 Shizi Street, Suzhou, 215006, China.
** Corresponding author. 96 Jinzhai Road, Hefei, 230026, China.
E-mail addresses: mahaitao@suda.edu.cn (H. Ma), rkhu@mail.ustc.edu.cn (R. Hu).
[1] Equal contribution.

https://doi.org/10.1016/j.canlet.2019.01.007
Received 13 September 2018; Received in revised form 10 December 2018; Accepted 8 January 2019

Abbreviations

SqCLC	squamous cell lung cancer
PDX	patient derived xenograft
BRD9	Bromodomain Containing 9
UTR	the untranslated region
FISH	Fluorescence In Situ Hybridization
IHC	Immunohistochemistry

cancers and has emerged as an attractive therapeutic target [12]. Although inhibition of BRD9 has shown profound anticancer and anti-inflammatory properties, the detailed function and mechanisms have not been determined, especially in SqCLC.

Here, we show that miR-140-3p is down regulated in SqCLC cells and tissues. Overexpression of miR-140-3p suppressed SqCLC cell growth and invasion. Moreover, BRD9 is a direct target of miR-140-3p. Inhibition of BRD9 remarkably reduced SqCLC tumorigenesis by downregulating c-myc. Restoration of BRD9 abolishes the function of miR-140-3p in SqCLC. Moreover, BRD9 correlated with clinical outcomes of SqCLC. These results indicate that miR-140-3p suppresses SqCLC tumorigenesis by targeting BRD9.

2. Materials and methods

2.1. Materials

BRD9, c-myc and GAPDH antibodies were purchased from Abcam (MA, USA). Keratinocyte-SFM, Bovine Pituitary Extract (BPE) and Epidermal Growth Factor (EGF) were purchased from Thermo Fisher Scientific (MA, USA). RPMI-1640, Fetal Bovine Serum (FBS), and Collagen I were purchased from Sigma-Aldrich (St. Louis, USA). BRD9 siRNAs and miR-140-3p mimics and inhibitors were obtained from GenePharma (Suzhou, China) (Table 1).

2.2. Cell culture

All SqCLC cell lines used in this study were obtained from ATCC and the cell library of the Chinese Academy of Sciences (Shanghai, China). HBEC3KT cells were cultured in Keratinocyte-SFM (GIBCO) supplemented with BPE and EGF (GIBCO) at 37 °C in 5% CO_2. HCC95, H226, H1703 and H2170 cells were cultured in RPMI-1640 (Sigma) with 10% FBS (Sigma) at 37 °C in 5% CO_2. Transfection of siRNAs, miRNA mimics and inhibitors was performed with Lipofectamine 2000 from Thermo Fisher Scientific (MA, USA).

For primary cells isolated from patient-derived xenografts (PDX), xenografts were minced and placed in 10% FBS containing DMEM with collagen IV (0.5 mg/ml, Sigma) and incubated at 37 °C for 60 min [13]. The dissociated suspension was filtered with a 100 μm strainer to obtain single cells that were then washed with culture medium. Primary cells were transfected with miR-140-3p mimics using the MISSION siRNA transfection reagent (Sigma).

2.3. Western blotting and immunohistochemistry

Cells were harvested and lysed in SDS lysis buffer (1% SDS, 10 mM HEPES, pH 7.0, 2 mM $MgCl_2$, universal nuclease 20 U/ml). Total cellular protein concentration was measured by the BCA assay kit (Thermo Fisher Scientific). Twenty μg protein samples were subjected to 10% SDS-PAGE and transferred to nitrocellulose blotting membranes (GE Healthcare). The membranes were blotted with primary antibodies (1:1000) overnight at 4 °C. The secondary antibody (1:5000) was incubated for 1 h at room temperature. Proteins were developed as previously described [14].

Immunohistochemistry (IHC) was performed according to our previous study [5]. Briefly, paraffin-embedded samples were deparaffinized and incubated with rabbit BRD9 antibody (1:200) for 1 h at 37 °C. After rinsing with PBS (pH 7.4), slides were treated with goat-anti-rabbit secondary antibody (1:3000) and incubated with 3-diaminobenzidine solution for 20 min.

2.4. Real-time qPCR

Total RNA was isolated from cells or tissues using TRIzol reagent (Thermo Fisher Scientific). Two μg total RNA was reverse transcribed using the SuperScript II reverse transcriptase kit (Thermo Fisher Scientific). Then, qPCR was performed using the power SYBR Green master mix (Thermo Fisher Scientific). The relative expression of mRNA was examined as the inverse log of the delta-delta CT and normalized to Actin. The primers were used as described in Table 1.

2.5. Clinical tumor samples

Fifty-two SqCLC tumor samples and twenty-two adjacent normal samples were collected from 52 patients from 2015 to 2018 at the First Affiliated Hospital of Soochow University. Pathological analysis confirmed that all tissues were indeed SqCLC (median age 67.19) (Table 2 and Table S1). All the specimens were obtained with informed consent from the patients, and this study was approved by the Ethics Committee of Soochow University.

2.6. Mammalian lentiviral overexpression vector construction

The coding sequence of BRD9 was amplified and cloned in the LV5 plasmid from GenePharma (Suzhou, China). LV5-GFP was used as a negative control. The primer sequences used against BRD9 are as follows: To generate lentiviral particles, plasmids were cotransfected into HEK293T cells along with the envelope (VSVG) and packaging (Delta 8.9) system using Lipofectamine 2000 (Thermo Fisher Scientific). The viral supernatants were filtered after two days of transfection. SqCLC cells were incubated with 8 μg/ml polybrene and virus. The efficiencies of overexpression were confirmed by Western blotting and real-time qPCR.

2.7. Cell proliferation and cell migration assay

Cell growth was measured using the Cell counting kit-8 (CCK8, Dojindo, Japan). The absorbance of each sample was measured at 450 nm. All experiments were performed in triplicate and the average

Table 1
Primer sequences for quantitative RT-PCR.

Gene	Forward Primer (5′-3′)	Reverse Primer (5′-3′)
BRD9	TGGGAGCTACAGCAAGAAAGT	CTGGAAGAGCGTCCTAGAGTG
c-myc	AAAGGCCCCCAAGGTAGTTA	GCACAAGAGTTCCGTAGCTG
GAPDH	CATGAGAAGTATGACAACAGCCT	AGTCCTTCCACGATACCAAAGT
miR-140-3p	CAGTGCTGTACCACAGGGTAGA	TATCCTTGTTCACGACTCCTTCAC
U6	CGCTTCGGCAGCACATATAC	TTCACGAATTTGCGTGTCATC

Table 2
Patient clinical characteristics.

Patient clinical characteristics		
Gender	Male	50 (96.2%)
	Female	2 (3.8%)
Age	≤60	11 (21.2%)
	> 60	41 (78.8%)
Smoking status	Yes	37 (71.2%)
	No	15 (28.8%)
Pathology grade	Stage I/II	41 (78.8%)
	Stage III	11 (21.2%)
T classification	T1/T2	37 (71.2%)
	T3/T4	15 (28.8%)
Lymph node	N0/N1	50 (96.2%)
	N1/N2	2 (3.8%)
Metastasis	M0	52 (100%)

values were calculated. The cell invasion assay was performed using cell culture insert membranes coated with Matrigel (BD Biosciences). Cells were starved and seeded into the upper chamber of the inserts (10^5 cells) in serum media. The low chamber was incubated with 10% FBS media. After 48 h, the cells were fixed and stained using 0.5% crystal violet.

2.8. 3′-UTR reporter assay

The BRD9 3′-UTR (untranslated region) and mutant variants were cloned into the pmirGLO reporter vector (Promega). Cells were co-transfected with pmirGLO-BRD9 wild-type or mutant plasmid and miR-140-3p mimics or negative controls (scramble). The luciferase activities were measured 24 h posttransfection using the dual-luciferase reporter assay kit (Promega) following the manufacturer's instructions.

2.9. PDX construction

Fresh SqCLC tumor tissue samples (patient ID: 1290024, Male, Age 55, F0) were kept on ice and processed in sterile conditions on the day of collection. Briefly, tumor tissues were cut into pieces and implanted subcutaneously into the interscapular fat pad of NOD/SCID mice (Vital River Laboratory Animal Technology, Beijing, China). These mice in the engraftment phase are called F1 mice. After the tumor reached approximately 1.5–2 cm (6–12 weeks), the additional transplant to F2, F3, etc., was prepared. In this study, F4 PDX models with tumor volumes of 50–150 mm^3 were used for downstream applications [13]. Tumor growth was monitored and calculated (width^2 x length)/2 at each time point. The mice were euthanized and tumors were photographed and stained with hematoxylin/eosin (H&E). All animal studies were approved and followed the guidelines of the animal ethics committee of Soochow University (Suzhou, China).

2.10. Meta-analysis and statistical analysis

For clinical data, miR-140-3p and BRD9 expression in the SqCLC in the Cancer Genome Atlas (TCGA) database was downloaded from UCSC (http://tcga.xenahubs.net). Kaplan-Meier analyses were performed using SPSS 22.0 (IBM Inc.) or generated using the online meta-analysis tool KM Plotter (http://kmplot.com/analysis/index.php?p=service) [15]. Significance tests and correlation analyses were performed using GraphPad Prism (GraphPad Software Inc.). The statistical significance of differences between groups was determined using ANOVA or two-tailed Student's t-test. A p-value less than 0.05 was considered statistically significant.

3. Results

3.1. MiR-140 is downregulated in SqCLC cell lines and clinical samples

MiR-140-3p expression levels were measured in normal lung cancer cell lines (HBEC3KT) and four squamous lung cancer cell lines, including HCC95, H226, H1703 and H2170. The results showed that miR-140-3p expression levels in SqCLC cell lines were significantly lower in

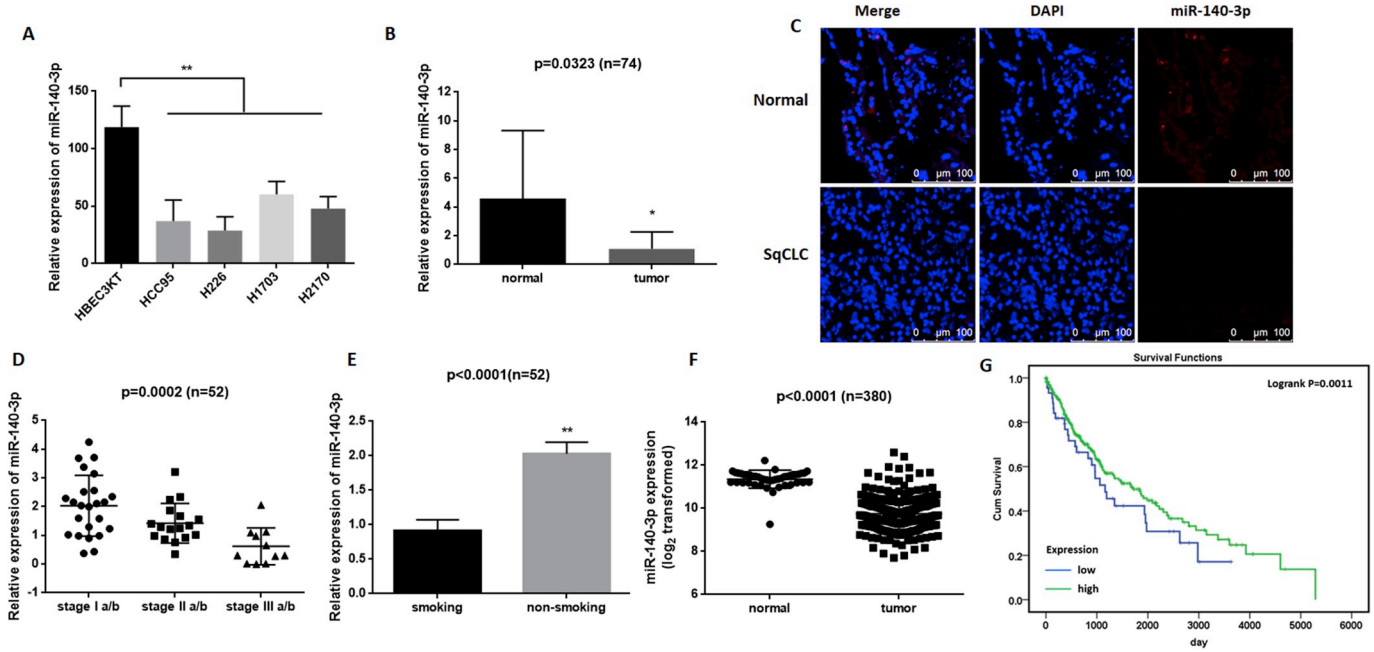

Fig. 1. miR-140-3p is downregulated in SqCLC cells and tissues. (A) Expression of miR-140-3p was analyzed by qRT-PCR in 4 SqCLC cell lines; HBEC3KT was set as a control. (B) The miR-140-3p level was downregulated in SqCLC tissues compared to normal samples using qRT-PCR (n = 74). (C) The expression of miR-140-3p in normal or SqCLC tissues was detected by FISH. (D) miR-140-3p expression in different clinical stages of SqCLC (n = 52). (E) MiR-140-3p expression in patients with or without smoking history. (F) TCGA data for miR-140-3p in SqCLC were analyzed (n = 380). (G) The survival rate was analyzed in 380 SqCLC patients with high or low expression of miR-140-3p. *p < 0.05, **p < 0.01 (Figure A, D, one-way ANOVA; Figure B, E, F, two-tailed Student's t-test). Experiments were performed at least in triplicate.

HBEC3KT (Fig. 1A). We next quantified the expression of miR-140-3p in 52 tumor samples and 22 normal tissues by qPCR and FISH. As seen in Fig. 1B and C, miR-140-3p levels in tumors were significantly lower than in normal tissues. It is also shown that the expression level of miR-140-3p in SqCLC patients is correlated with later TNM stages (Fig. 1D) and smoking status (Fig. 1E). In addition, we validated these findings using a validation cohort of 380 patient samples from the TCGA database (https://xenabrowser.net/datapages/?hub=https://tcga.xenahubs.net:443). In conjunction with our qPCR expression data, miR-140-3p was also significantly lower in most tumors compared to normal tissues (Fig. 1F). In addition, the survival rate from these TCGA data was analyzed; as seen in Fig. 1G, patients with low miR-140-3p have worse outcomes. These results demonstrate that miR-140-3p is downregulated in SqCLC and can serve as a prognostic biomarker for SqCLC.

3.2. MiR-140-3p suppresses tumorigenesis of SqCLC in vitro and in vivo

To investigate the function of miR-140-3p in the growth of squamous lung cancer tumors, miR-140-3p mimics or the scramble controls were transfected into H226 cells and HCC95 cells (Fig. 2A). As shown in Fig. 2B and C, miR-140-3p inhibited cell growth posttransfection. Meanwhile, the expression of miR-140-3p suppressed the invasion of H226 and HCC95 cells by more than 70% and 55%, respectively (Fig. 2D and E). Furthermore, to determine whether miR-140-3p is involved in tumorigenesis in a clinical model (patient ID:1290024; Male, Age 55), patient-derived xenografts (PDX) were established in NOD/SCID mice. First, the primary cells from PDX models were digested and transfected with miR-140-3p or mimic controls. As predicted, PDX cell growth was inhibited by miR-140-3p (Fig. 3A and B). In addition, tumors in the PDX models were intratumoral injected with 2OD miR-140-3p twice a week. As shown in Fig. 3C–F and Fig. S1, miR-140-3p significantly suppressed the tumor growth of SqCLC PDX. These results indicate that miR-140-3p acts as a tumor suppressor in squamous lung cancer both in vitro and in vivo.

3.3. MiR-140-3p directly targets the 3′UTR of BRD9

To further elucidate the function of miR-140-3p in regulating the tumorigenesis of SqCLC, we examined the oncogenes possibly targeted by miR-140-3p. Using the bioinformatics tools TargetScan, miRBase and miRDB, we identified BRD9 as one of the putative targets of miR-140-3p (Fig. 4A). Next, the 3′UTR fragment of BRD9 was cloned downstream of a luciferase reporter system in the pmirGLO vector. Subsequently, we performed luciferase reporter assays to examine the relationship between miR-140-3p and BRD9. As shown in Fig. 4B and C, the reporter with wild type BRD9 3′UTR had lower luciferase activity in two SqCLC cells expressing miR-140-3p compared to the luciferase activity in the control group. In addition, the inhibition of luciferase activity by miR-140-3p was abolished by the mutant BRD9 3′UTR (Fig. 4B and C). To further validate the association between miR-140-3p and BRD9, we detected endogenous BRD9 mRNA and protein levels in two SqCLC cells after transfection with miR-140-3p mimics or scramble

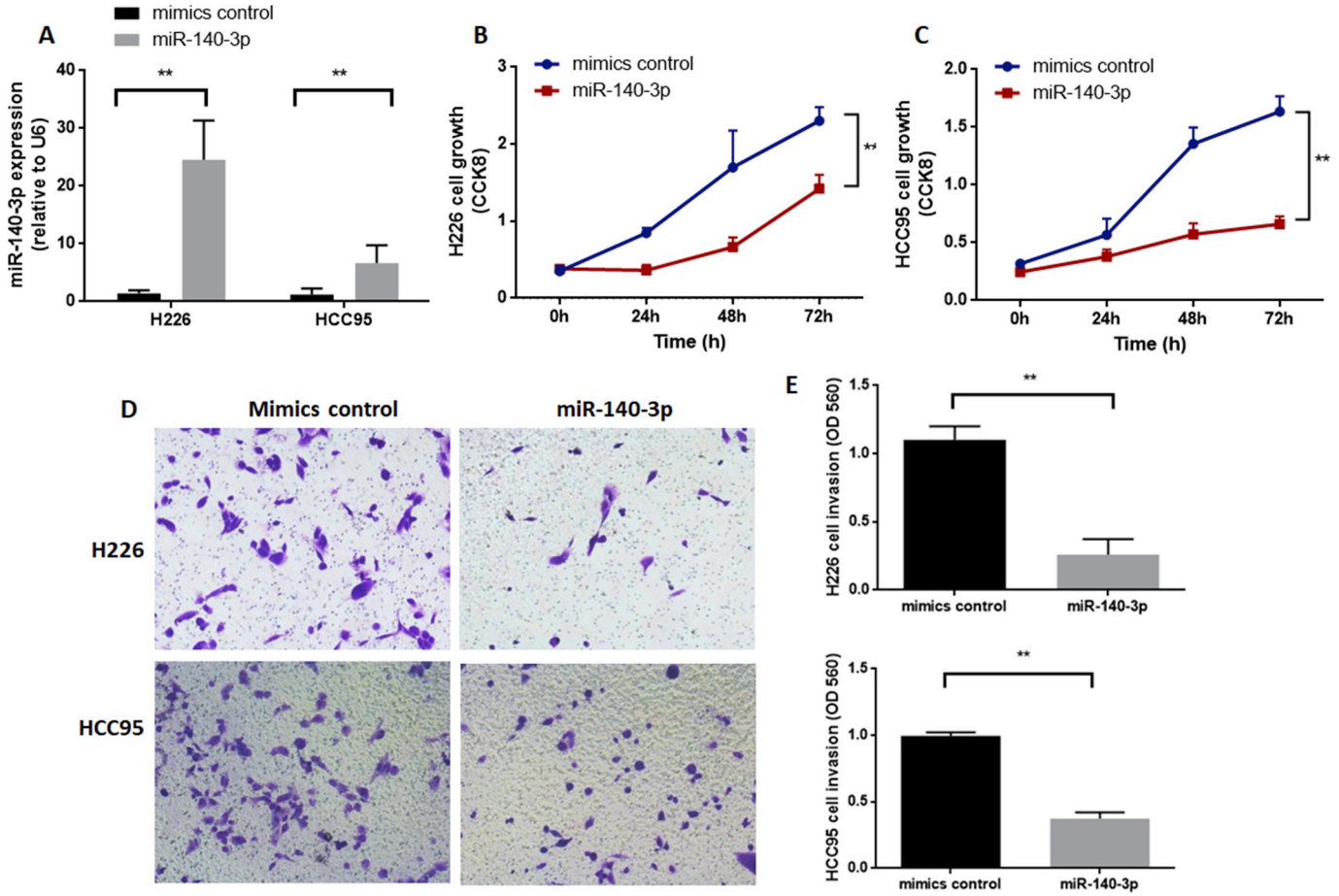

Fig. 2. miR-140-3p suppresses the growth and invasion of SqCLC cells. After transfection with miR-140-3p mimics, (A) the expression of miR-140-3p in two SqCLC cell lines was detected by qRT-PCR. Cell proliferation of H226 (B) and HCC95 (C) cells was detected by CCK8. (D) Cell invasion after transfection with miR-140-3p was measured and cells were stained with crystal violet. (E) Crystal violet was dissolved in 33% acetic acid, and the absorbance at 560 nm was measured in three independent experiments (n = 3). *p < 0.05, **p < 0.01 (Figure A, one-way ANOVA; Figure E, two-tailed Student's t-test). (For interpretation of the references to colour in this figure legend, the reader is referred to the Web version of this article.)

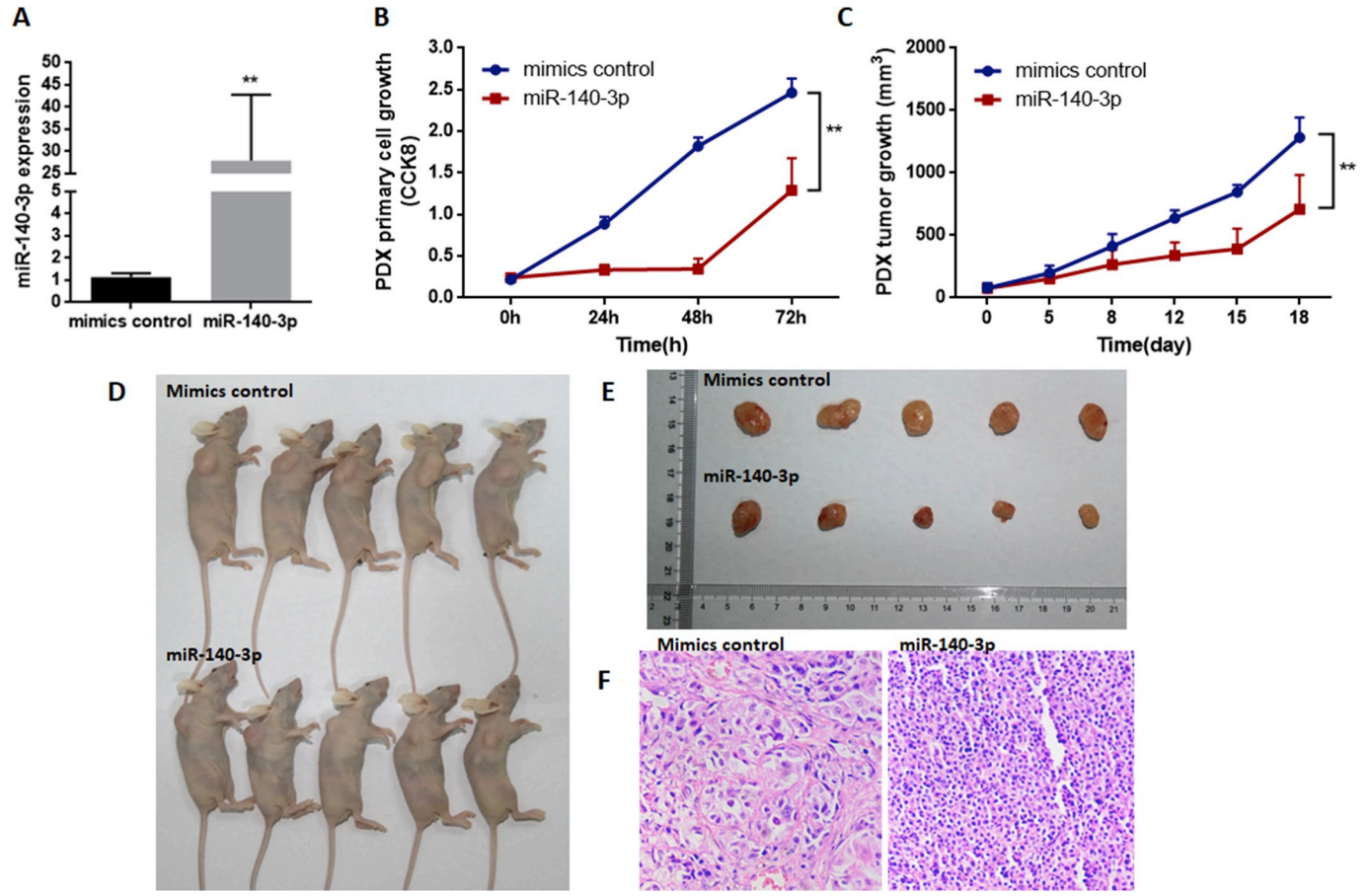

Fig. 3. miR-140-3p inhibits SqCLC PDX growth both in vitro and in vivo. (A) Patient derived xenografts (PDX) of SqCLC were digested and the primary cells were transfected with miR-140-3p. (B) Primary cell proliferation was measured using the CCK8 kit. (C) PDX models were intratumoral injected with 2OD miR-140-3p or mimics twice a week and tumor growth was measured twice a week (n = 5). (D) and (E) PDX tumors were photographed. (F) The PDX tumors were stained with hematoxylin and eosin (H&E). *p < 0.05, **p < 0.01 (one-way ANOVA). Experiments were performed at least in triplicate.

controls. As shown in Fig. 4D–F, the level of BRD9 mRNA and protein was decreased by miR-140-3p. Taken together, these results suggest that BRD9 is a direct target of miR-140-3p.

3.4. BRD9 regulates the growth and invasion of SqCLC cells

BRD9 is frequently overexpressed in several types of cancer, especially in myeloid leukemia (AML). Previous studies indicated that BRD9 was required to sustain c-myc transcription in AML [12,16], but the linkage of BRD9 and c-myc is still unknown in SqCLC. Towards this end, we examined cellular phenotypes after knocking down BRD9 with two siRNAs. The BRD9 level was detected via qPCR and Western blotting. Depletion of BRD9 led to an inhibition of c-myc activity both at the protein level (Fig. 5A and Fig. S2) and the mRNA level (Fig. 5B and C). In addition, knockdown of BRD9 led to a striking inhibition of proliferation and invasion in SqCLC cells (Fig. 5D–F, Fig. S3), which was consistent with the reduced c-myc pathway. These results indicate that BRD9 acts as an oncogene and promotes the proliferation and invasion of SqCLC by regulating c-myc.

3.5. BRD9 counteracts the function of miR-140-3p

To study whether miR-140-3p exerts its effects through BRD9, we overexpressed BRD9 in H226 cells via lentiviral infection. This construct was lacking the 3′UTR, so miR-140-3p could not affect its expression. As a result, pLenti-BRD9 could restore the expression of BRD9 both at the mRNA and protein level (Figs. 6A-C and S4), which in turn stimulates c-myc expression. Furthermore, restoration of BRD9 abolished the negative impact on cell proliferation and cell invasion by miR-140-3p (Fig. 6D–F). These results show that BRD9 is a direct functional target of miR-140-3p and that miR-140-3p functions as a tumor suppressor through regulating BRD9.

3.6. BRD9 is a diagnostic and prognostic biomarker of squamous lung cancer

The expression levels of BRD9 in SqCLC clinical samples were examined. As shown in Fig. 7A, BRD9 mRNA levels were much higher in tumor samples (n = 74). As predicted, the levels of BRD9 in 52 SqCLC patients were associated with the clinical stage of the disease (Fig. 7B), but no correlation was observed between BRD9 expression and smoking history (Fig. S5). An interesting result was that the expression of BRD9 was negatively correlated with the expression of miR-140-3p (Fig. 7C). In addition, the BRD9 protein level in patients was measured with IHC and the score was valued (Fig. 7D and E). The BRD9 protein level was much higher in tumor tissues compared to normal controls. Furthermore, we applied bioinformatics analysis to a larger data set from TCGA (https://xenabrowser.net/datapages/?hub=https://tcga.xenahubs.net:443). As shown in Fig. 7F, BRD9 expression was substantially higher in 553 SqCLC patients compared to the normal control. In addition, we performed a survival meta-analysis based on BRD9 expression. A Kaplan-Meier curve was generated using the online meta-analysis tool. From the analysis of gene expression and clinical data for 1926 lung cancer patients, we found that high expression of BRD9 predicts worse outcomes in patients (Fig. 7G), suggesting that BRD9 is a diagnostic and prognostic biomarker for squamous lung cancer.

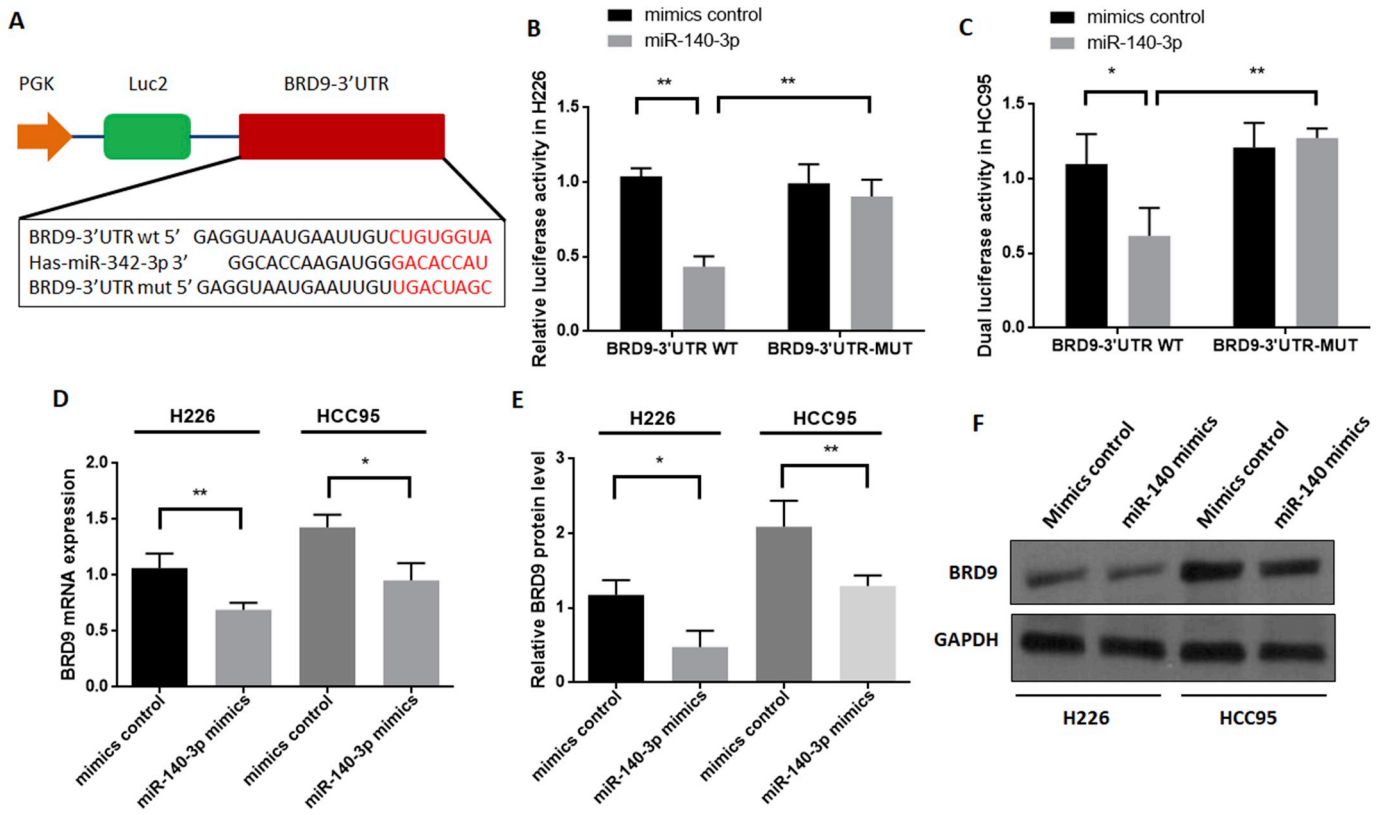

Fig. 4. miR-140-3p directly targets BRD9. (A) The miR-140-3p-binding site located on the 3′UTR of BRD9 mRNA in the wild type or mutants of BRD9 3′UTR were cloned into the pmirGLO plasmid. (B) and (C) miR-140-3p mimics or scramble controls and wild-type or mutant BRD9 3′UTR were cotransfected into H226 and HCC95 cells separately. MiR-140-3p reduced luciferase activities in cells transfected with the wild-type 3′UTR but did not alter luciferase activities in cells transfected with the mutant BRD9 3′UTR. (D) MiR-140-3p decreased BRD9 mRNA expression in H226 and HCC95 cells. (E) and (F) Western blotting was performed after transfecting cells with miR-140-3p mimics or mimic controls, and BRD9 protein levels were detected in three independent experiments. *p < 0.05, **p < 0.01 compared to the corresponding controls (two-tailed Student's t-test).

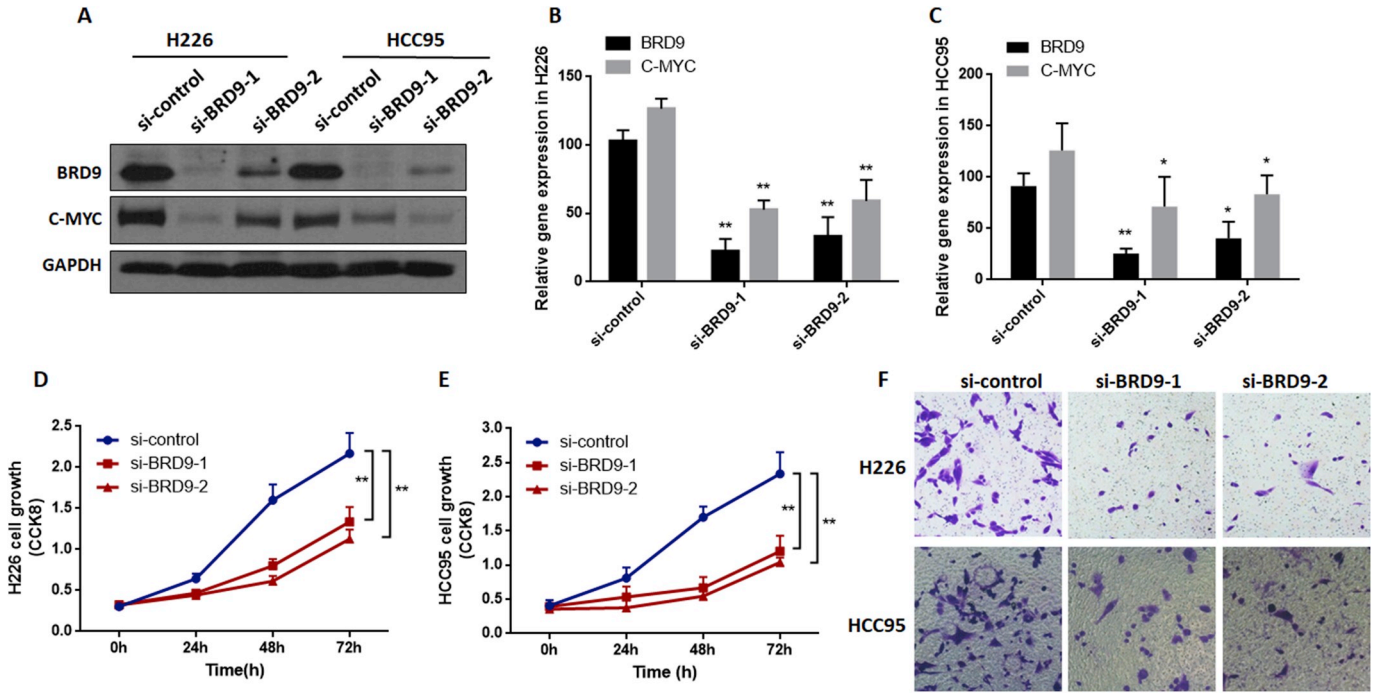

Fig. 5. BRD9 regulates the growth and invasion of SqCLC cells. BRD9 was downregulated by two siRNA in H226 and HCC95 cells, and the protein levels of BRD9 and c-myc were measured in three independent experiments (A). The mRNA levels of BRD9 and c-myc were detected by qRT-PCR (B and C). H226 and HCC95 cell growth was assessed in three independent experiments (D and E) (n = 3, **p < 0.01). Cell invasion in two SqCLC cell lines was analyzed using the transwell assay (F) (n = 3). *p < 0.05, **p < 0.01 compared to the corresponding controls (one-way ANOVA).

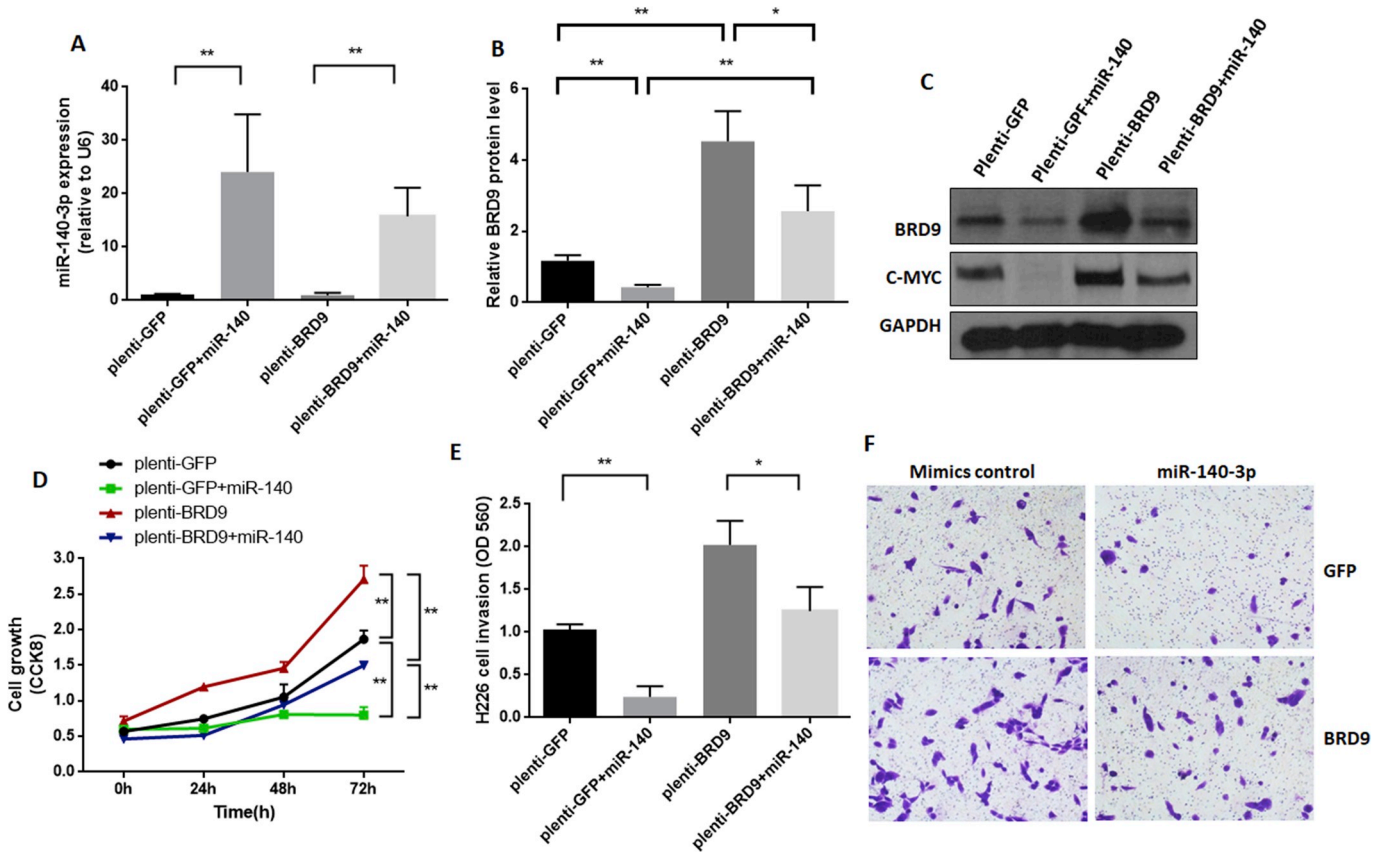

Fig. 6. BRD9 counteracted the suppressive effect of miR-140-3p. (A) qRT-PCR was used to analyze the expression of miR-140-3p in each group of transfected cells. (B) and (C) Western blotting confirmed that restoration of BRD9 in H226 cells can counteract the effects of miR-140-3p. (D) to (F) Overexpression of BRD9 rescued cell proliferation and invasion as shown by CCK8 and transwell assays. n > 3, *p < 0.05, **p < 0.01 compared to the corresponding controls (one-way ANOVA).

4. Discussion

Cell proliferation and invasion are two key factors leading to the malignant tumorigenesis observed in cancer. Targeting these two aspects is a potential approach in SqCLC therapy. Several studies have reported that miRNAs play important roles in lung cancer, which may be very valuable in the diagnosis and treatment of this malignant disease. Accumulating evidence indicates that miRNAs, including miR-17-5p, miR-140-3p, and let-7, are involved in the progression and invasion of non-small cell lung cancer (NSCLC) [17,18]. However, the mechanism of miR-140-3p-mediated regulation in SqCLC remains unclear.

In this study, we investigated the roles and mechanisms of miR-140-3p, BRD9 and c-myc in SqCLC. We found that SqCLC is associated with a low expression of miR-140-3p both in cell lines and in clinical samples. Overexpression of miR-140-3p inhibits SqCLC cell proliferation and invasion. To further demonstrate the clinical importance of miR-140-3p, we constructed several lines of patient-derived xenografts (PDX). As a result, miR-140-3p suppresses the primary cell proliferation extracted from PDX and inhibits PDX tumor growth.

To explore the detailed mechanism by which pathways are involved in the function of miR-140-3p in SqCLC, bioinformatics analysis was used to predict a relationship between miR-140-3p and BRD9. As we predicted, miR-140-3p directly targeted BRD9 and suppressed BRD9 expression in both HCC95 and H226 cells (Fig. 4). BRD9 is a bromodomain-containing protein, a subunit of the BAF (SWI/SNF) complex, which plays a role in acetyl-lysine recognition. Several studies revealed that inhibition of BRD9 suppressed tumor growth, prompting a cytostatic response [12,19]. There are already some inhibitors produced that target this attractive therapeutic protein in cancer. Beyond its presence in the BAF complex, the function of BRD9 remains unknown. Our results indicated that knockdown of BRD9 suppressed cell proliferation and invasion in SqCLC cells and primary PDX cells. Although a linkage between BRD9 and c-myc was unveiled in previous studies in AML [20], it remains unconfirmed in SqCLC. In our study, an interesting result was that downregulation of BRD9 led a degradation of c-myc. C-myc is a “master regulator”, which controls many aspects of tumor cell growth and cellular metabolism. Accumulated evidence confirmed that c-myc is increased, resulting in mitosis, and acts as a classic proto-oncogene, contributing to the tumorigenesis of non-small cell lung cancer. C-myc was always overexpressed in human lung cancer cell lines and patients, and patients with c-myc positive tumors had a short survival time compared to c-myc negative patients [21,22]. Consistent with previous reports, c-myc was also highly expressed in most tumor tissues both in our clinical cohort and in the TCGA database (Fig. S6).

Furthermore, we performed rescue experiments by overexpressing BRD9 in SqCLC cells and incubation of miR-140-3p. These data indicate that BRD9 could counteract some effects of miR-140-3p on proliferation and invasion in SqCLC cells, suggesting that miR-140-3p modulates tumorigenesis mainly by targeting BRD9. In addition, BRD9 expression was negatively correlated with miR-140-3p levels in both SqCLC samples and the TCGA database. Meanwhile, BRD9 expression was correlated with clinical information, including tumor size and tumor stage. Consistent with the knowledge that smoking decreases global miRNA expression, miR-140-3p was also reduced in smoking patients in our cohort data (Fig. 1E) [23,24]. However, unlike miR-140-3p, BRD9 expression was not associated with smoking status that may be caused by other pathways involved in BRD9 expression and function, such as the SWI/SNF complex [10]. A comprehensive meta-analysis revealed that patients with high levels of BRD9 in their tumors have a worse

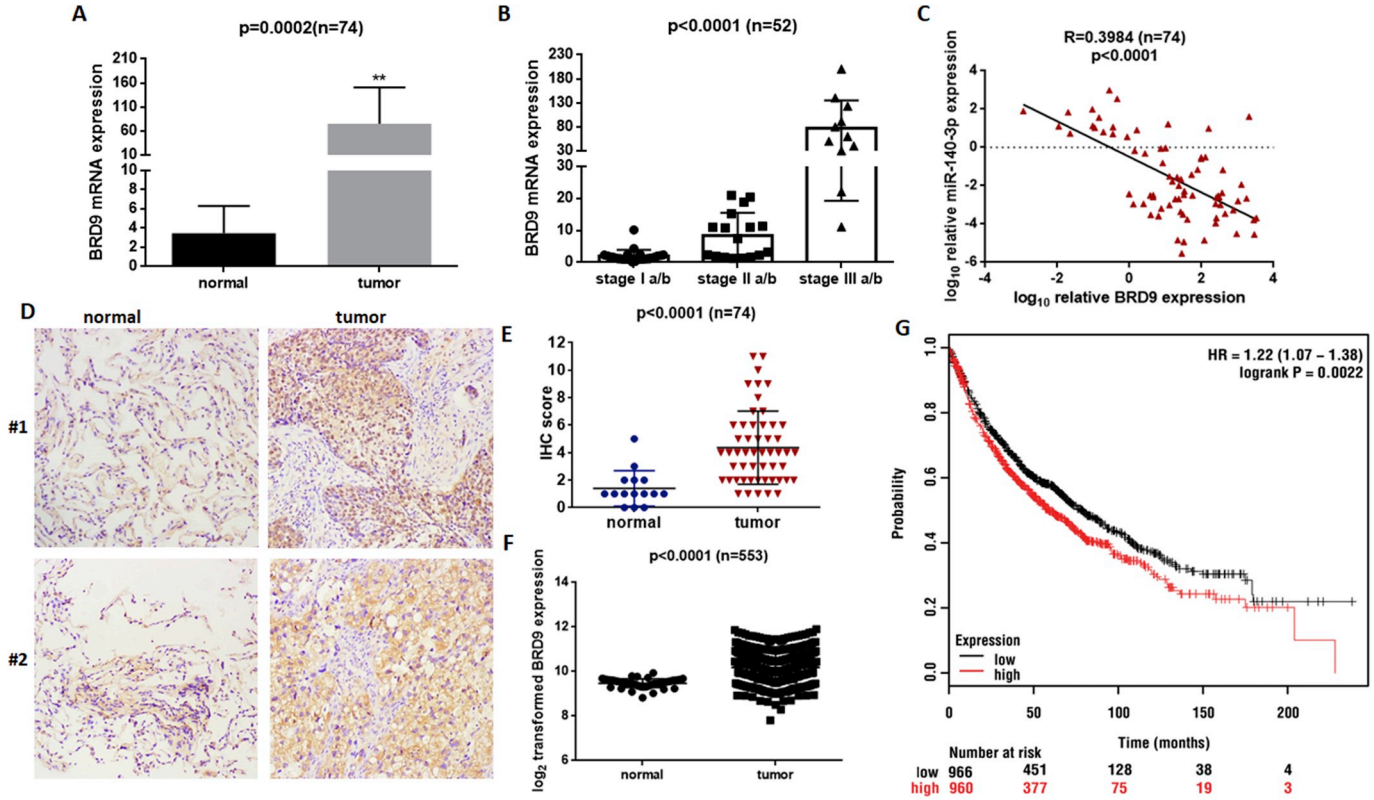

Fig. 7. BRD9 level is a prognostic biomarker in SqCLC tissues. QRT-PCR was used to analyze the expression of BRD9 in 52 SqCLC patients and 22 normal lung tissues, which is upregulated in SqCLC samples (A). BRD9 expression was upregulated in the late stage of SqCLC patients (B). (C) The expression of BRD9 is negatively correlated with miR-140-3p. (D) The expression of BRD9 protein levels was measured with IHC. (E) The score of IHC in 74 samples was evaluated. (F) TCGA data for 553 SqCLC patient samples were analyzed. (G) Kaplan-Meier plots were constructed for 1926 NSCLC patients stratified by the expression of BRD9. *p < 0.05, **p < 0.01 (one-way ANOVA).

prognosis.

In summary, we demonstrated, for the first time, that miR-140-3p inhibited SqCLC proliferation and invasion in vitro and in vivo by targeting BRD9. BRD9 is an oncogene that promotes SqCLC tumorigenesis by regulating c-myc. Clinical information suggested that miR-140-3p and BRD9 may be used as prognostic and diagnostic biomarkers. These results also revealed a new regulatory network involving miR-140-3p and BRD9, which may be implemented in the therapeutic treatment of SqCLC in the future.

Disclosure statement

The authors have no conflict of interest to declare.

Contributors

H.H., Y.W. and Q.L. performed the experiments and collected the clinical samples, analyzed the data and wrote the manuscript. X.F. analyzed the data and modified the manuscript. H.M. and R.H. designed and supervised the work and wrote the manuscript. All the authors are in agreement with the content of the manuscript.

Conflicts of interest

The authors declare that they have no competing interests.

Acknowledgements

This work was supported by grants from the National Natural Science Foundation of China (81672281and 31300746), the Jiangsu Science and Technology project (BE2015638), the Suzhou Science and Technology project (ZXL2018171) and the National Key Research and Development program of China (2016YFC0904303). We also thank John D. Minna, Kenneth E. Huffman, Yajie Zhang and Yonghao Yu from the University of Texas Southwestern Medical center for advice and cell lines.

Appendix A. Supplementary data

Supplementary data to this article can be found online at https://doi.org/10.1016/j.canlet.2019.01.007.

References

[1] J. Brahmer, K.L. Reckamp, P. Baas, L. Crino, W.E. Eberhardt, E. Poddubskaya, S. Antonia, A. Pluzanski, E.E. Vokes, E. Holgado, D. Waterhouse, N. Ready, J. Gainor, O. Aren Frontera, L. Havel, M. Steins, M.C. Garassino, J.G. Aerts, M. Domine, L. Paz-Ares, M. Reck, C. Baudelet, C.T. Harbison, B. Lestini, D.R. Spigel, Nivolumab versus docetaxel in advanced squamous-cell non-small-cell lung cancer, N. Engl. J. Med. 373 (2015) 123–135.

[2] S. Ramalingam, C. Belani, Systemic chemotherapy for advanced non-small cell lung cancer: recent advances and future directions, Oncologist 13 (Suppl 1) (2008) 5–13.

[3] S.A. Khuder, Effect of cigarette smoking on major histological types of lung cancer: a meta-analysis, Lung Canc. 31 (2001) 139–148.

[4] X.H. Liu, Z.L. Liu, M. Sun, J. Liu, Z.X. Wang, W. De, The long non-coding RNA HOTAIR indicates a poor prognosis and promotes metastasis in non-small cell lung cancer, BMC Canc. 13 (2013) 464.

[5] X. Xue, X. Fei, W. Hou, Y. Zhang, L. Liu, R. Hu, miR-342-3p suppresses cell proliferation and migration by targeting AGR2 in non-small cell lung cancer, Cancer Lett. 412 (2018) 170–178.

[6] D. Chen, W. Guo, Z. Qiu, Q. Wang, Y. Li, L. Liang, L. Liu, S. Huang, Y. Zhao, X. He, MicroRNA-30d-5p inhibits tumour cell proliferation and motility by directly targeting CCNE2 in non-small cell lung cancer, Cancer Lett. 362 (2015) 208–217.

[7] S. Langsch, U. Baumgartner, S. Haemmig, C. Schlup, S.C. Schafer, S. Berezowska, G. Rieger, P. Dorn, M.P. Tschan, E. Vassella, miR-29b mediates NF-kappaB signaling in KRAS-induced non-small cell lung cancers, Cancer Res. 76 (2016) 4160–4169.

[8] W.B. Xie, L.H. Liang, K.G. Wu, L.X. Wang, X. He, C. Song, Y.Q. Wang, Y.H. Li, MiR-

140 expression regulates cell proliferation and targets PD-L1 in NSCLC, Cell. Physiol. Biochem. 46 (2018) 654–663.
[9] X. Tan, W. Qin, L. Zhang, J. Hang, B. Li, C. Zhang, J. Wan, F. Zhou, K. Shao, Y. Sun, J. Wu, X. Zhang, B. Qiu, N. Li, S. Shi, X. Feng, S. Zhao, Z. Wang, X. Zhao, Z. Chen, K. Mitchelson, J. Cheng, Y. Guo, J. He, A 5-microRNA signature for lung squamous cell carcinoma diagnosis and hsa-miR-31 for prognosis, Clin. Canc. Res. 17 (2011) 6802–6811.
[10] D. Remillard, D.L. Buckley, J. Paulk, G.L. Brien, M. Sonnett, H.S. Seo, S. Dastjerdi, M. Wuhr, S. Dhe-Paganon, S.A. Armstrong, J.E. Bradner, Degradation of the BAF complex factor BRD9 by heterobifunctional ligands, Angew Chem. Int. Ed. Engl. 56 (2017) 5738–5743.
[11] R.M. Karim, E. Schonbrunn, An advanced tool to interrogate BRD9, J. Med. Chem. 59 (2016) 4459–4461.
[12] A.F. Hohmann, L.J. Martin, J.L. Minder, J.S. Roe, J. Shi, S. Steurer, G. Bader, D. McConnell, M. Pearson, T. Gerstberger, T. Gottschamel, D. Thompson, Y. Suzuki, M. Koegl, C.R. Vakoc, Sensitivity and engineered resistance of myeloid leukemia cells to BRD9 inhibition, Nat. Chem. Biol. 12 (2016) 672–679.
[13] I. Fichtner, J. Rolff, R. Soong, J. Hoffmann, S. Hammer, A. Sommer, M. Becker, J. Merk, Establishment of patient-derived non-small cell lung cancer xenografts as models for the identification of predictive biomarkers, Clin. Canc. Res. 14 (2008) 6456–6468.
[14] X. Xue, X. Wang, Y. Zhao, R. Hu, L. Qin, Exosomal miR-93 promotes proliferation and invasion in hepatocellular carcinoma by directly inhibiting TIMP2/TP53INP1/CDKN1A, Biochem. Biophys. Res. Commun. 502 (2018) 515–521.
[15] B. Gyorffy, P. Surowiak, J. Budczies, A. Lanczky, Online survival analysis software to assess the prognostic value of biomarkers using transcriptomic data in non-small-cell lung cancer, PLoS One 8 (2013) e82241.
[16] L.J. Martin, M. Koegl, G. Bader, X.L. Cockcroft, O. Fedorov, D. Fiegen, T. Gerstberger, M.H. Hofmann, A.F. Hohmann, D. Kessler, S. Knapp, P. Knesl, S. Kornigg, S. Muller, H. Nar, C. Rogers, K. Rumpel, O. Schaaf, S. Steurer, C. Tallant, C.R. Vakoc, M. Zeeb, A. Zoephel, M. Pearson, G. Boehmelt, D. McConnell, Structure-based design of an in vivo active selective BRD9 inhibitor, J. Med. Chem. 59 (2016) 4462–4475.
[17] M. Raponi, L. Dossey, T. Jatkoe, X. Wu, G. Chen, H. Fan, D.G. Beer, MicroRNA classifiers for predicting prognosis of squamous cell lung cancer, Cancer Res. 69 (2009) 5776–5783.
[18] M.S. Kumar, S.J. Erkeland, R.E. Pester, C.Y. Chen, M.S. Ebert, P.A. Sharp, T. Jacks, Suppression of non-small cell lung tumor development by the let-7 microRNA family, Proc. Natl. Acad. Sci. U. S. A. 105 (2008) 3903–3908.
[19] M. Perez-Salvia, M. Esteller, Bromodomain inhibitors and cancer therapy: from structures to applications, Epigenetics 12 (2017) 323–339.
[20] K.F. Kramer, N. Moreno, M.C. Fruhwald, K. Kerl, BRD9 inhibition, alone or in combination with cytostatic compounds as a therapeutic approach in rhabdoid tumors, Int. J. Mol. Sci. 18 (2017).
[21] J. Yoo, C.H. Kim, S.H. Song, B.Y. Shim, Y.J. Jeong, M.I. Ahn, S. Kim, D.G. Cho, M.S. Jo, K.D. Cho, H.J. Cho, S.J. Kang, H.K. Kim, Expression of caspase-3 and c-myc in non-small cell lung cancer, Canc. Res. Treat. 36 (2004) 303–307.
[22] C.D. Little, M.M. Nau, D.N. Carney, A.F. Gazdar, J.D. Minna, Amplification and expression of the c-myc oncogene in human lung cancer cell lines, Nature 306 (1983) 194–196.
[23] G. Wang, R. Wang, Y. Strulovici-Barel, J. Salit, M.R. Staudt, J. Ahmed, A.E. Tilley, J. Yee-Levin, C. Hollmann, B.G. Harvey, R.J. Kaner, J.G. Mezey, S. Sridhar, S.G. Pillai, H. Hilton, G. Wolff, H. Bitter, S. Visvanathan, J.S. Fine, C.S. Stevenson, R.G. Crystal, Persistence of smoking-induced dysregulation of miRNA expression in the small airway epithelium despite smoking cessation, PLoS One 10 (2015) e0120824.
[24] J.W. Graff, L.S. Powers, A.M. Dickson, J. Kim, A.C. Reisetter, I.H. Hassan, K. Kremens, T.J. Gross, M.E. Wilson, M.M. Monick, Cigarette smoking decreases global microRNA expression in human alveolar macrophages, PLoS One 7 (2012) e44066.